# The influence of sediment cover variability on long-term river incision rates: An example from the Peikang River, central Taiwan

Brian J. Yanites,[1,2] Gregory E. Tucker,[1,3] Han-Lun Hsu,[4] Chien-chih Chen,[4] Yue-Gau Chen,[5] and Karl J. Mueller[1]

Received 24 November 2010; revised 6 May 2011; accepted 23 May 2011; published 24 August 2011.

[1] This study explores the hypothesis that the relative frequency of rock exposure in the bed of an incising channel can have a first-order impact on the long-term average erosion rate. The 1999 Chi-Chi earthquake in central Taiwan generated thousands of landslides along the middle reach of the Peikang River. Sediment from these landslides produced widespread aggradation, such that much of the river's bed remains shielded from active bedrock incision. We present data that constrain the spatial and temporal variability of sediment cover for the Peikang River. Because the river is undergoing spatially variable Holocene bedrock incision (1–10 mm/yr), it offers a unique natural experiment to test the influence of intermittent sedimentation on long-term incision rates. Published electrical resistivity surveys at seven locations along the river reveal median sediment depth values ranging from 1.9 to 11.5 m. The sediment depth correlates inversely with long-term incision rate and sediment transport capacity. We interpret this as an indication that the frequency of bedrock exposure exerts a major influence on incision along the Peikang River.

**Citation:** Yanites, B. J., G. E. Tucker, H.-L. Hsu, C. Chen, Y.-G. Chen, and K. J. Mueller (2011), The influence of sediment cover variability on long-term river incision rates: An example from the Peikang River, central Taiwan, *J. Geophys. Res.*, *116*, F03016, doi:10.1029/2010JF001933.

## 1. Introduction

[2] The dynamics of fluvial incision represent a critical link between tectonic and climatic processes. Although channels cover only a small percent of geographical area in a drainage basin, their incision sets the local base level for hillslopes, which produce sediment that is then carried by the rivers. As the sediment is transported by the river, it can influence incision processes in two ways: (1) by acting as 'tools' that abrade and fracture the underlying bedrock, or (2) by acting as a shield, protecting the bedrock from all erosive processes [*Gilbert*, 1877; *Lamb et al.*, 2008; *Sklar and Dietrich*, 2004]. Many processes can erode bedrock on a riverbed [*Whipple et al.*, 2000]; however, the role of sediment cover inhibiting potential erosive events is increasingly recognized as an important control on bedrock river dynamics [*Hartshorn et al.*, 2002; *Finnegan et al.*, 2007; *Johnson and Whipple*, 2007; *Johnson et al.*, 2009; *Korup and Montgomery*, 2008; *Turowski et al.*, 2007, 2008a; *Lague*, 2010; *Yanites and Tucker*, 2010]. Because sediment supply and cover are ultimately tied to hillslope erosion, a strong coupling between channel and hillslope processes exists. We explore this coupling as we document the spatial and temporal variability of sediment cover along the Peikang River in central Taiwan.

[3] Landsliding and other hillslope activity are temporally variable and often driven by large earthquakes or storms [*Benda and Dunne*, 1997; *Dadson et al.*, 2004; *Meunier et al.*, 2007], and it is thus likely that sediment cover in rivers varies over time. As material from sediment-delivery events travels through the fluvial system, it can cover the underlying bedrock and slow the rate of incision. This causes temporal variability in erosion rate that is controlled by the variability in sediment supply. It is thus necessary to understand, acknowledge, and document sediment cover variability in order to properly model bedrock river evolution [e.g., *Lague*, 2010].

[4] A number of flume studies have shown evidence supporting the notion that sediment cover controls bedrock river erosion [*Shepherd*, 1972; *Shepherd and Schumm*, 1974; *Sklar and Dietrich*, 2001; *Finnegan et al.*, 2007; *Johnson and Whipple*, 2007; *Chatanantavet and Parker*, 2008; *Johnson and Whipple*, 2010]. Short-term measurements of the distribution of erosion in real rivers also point to an important role of sediment cover in Taiwan [*Hartshorn et al.*, 2002; *Turowski et al.*, 2008b; *Johnson et al.*, 2010]. Recent mor-

[1]Department of Geological Sciences, University of Colorado at Boulder, Boulder, Colorado, USA.
[2]Now at Department of Geological Sciences, University of Michigan, Ann Arbor, Michigan, USA.
[3]CIRES, Boulder, Colorado, USA.
[4]Institute of Geophysics, National Central University, Jhongli, Taiwan.
[5]Department of Geosciences, National Taiwan University, Taipei, Taiwan.


0148-0227/11/2010JF001933

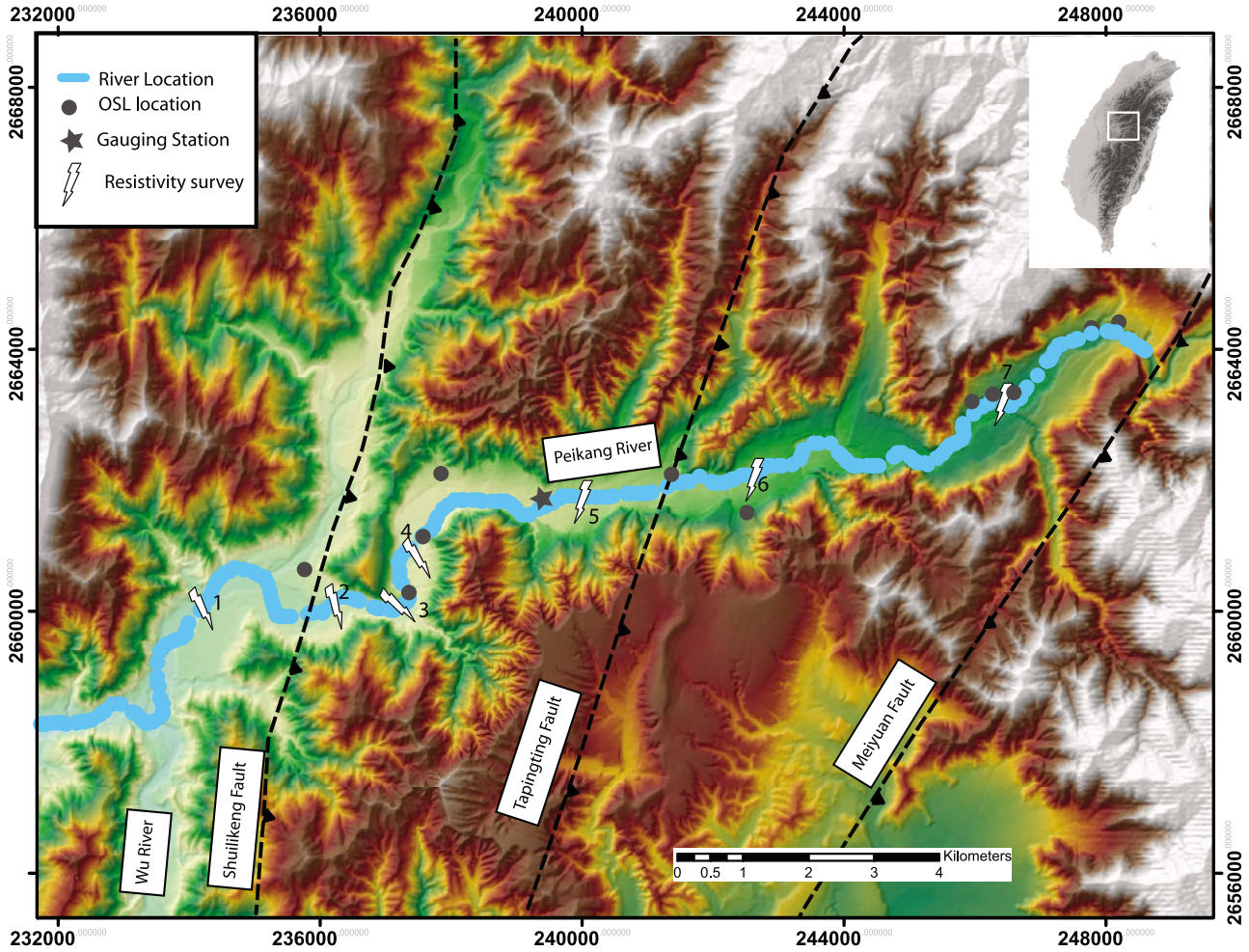


**Figure 1.** Digital elevation model draped over a shaded relief image of the study reach along the Peikang River. White lightning bolts represent electrical resistivity locations. Grey triangles are OSL sample locations. Black star is gauging station 1430H032. Fault locations from *Powell* [2003].

phologic studies also suggest that sediment cover is important on geologic timescales, but data sets linking morphology, sediment cover, and long-term incision are limited to only a few locations [*Cowie et al.*, 2008*; Finnegan et al.*, 2008].

[5] In this work, we document spatial and temporal changes of sediment cover along a bedrock river in central Taiwan. We test the hypothesis that sediment cover variability (in both space and time) plays a central role in modulating long-term fluvial incision rates [*Bull*, 1979; *Sklar and Dietrich*, 2004; *Turowski et al.*, 2007; *Lague*, 2010]. To do this, we constrain transport capacity, incision rate, and sediment cover. Measurement of sediment cover reveals that in some reaches bedrock erosion has ceased, and in others it has significantly slowed, as the river responds to a sudden increase in sediment flux set off by the 1999 Chi-Chi earthquake. However, Holocene incision rates require that these reaches erode at long-term rates of ~1–10 mm/yr. Our results suggest that spatial and temporal variations in sediment supply are necessary to produce the observed pattern of incision along the Peikang River. Given the limitations of short-term measurements of sediment cover, we suggest that sediment depth offers a proxy of the relative long-term effect of sediment cover along a reach undergoing differential incision.

## 2. Study Area

[6] We focus on the Peikang River of central Taiwan. Located just to the north of the Puli basin, the river crosses several active thrust faults of the western part of the island (Figure 1). A reach between the Meiyuan Fault and the confluence with the Wu River is undergoing differential incision over the Holocene as it passes over the active Shuilikeng fault [*Yanites et al.*, 2010a]. The incision rate pattern mimics estimates of basal shear stress, suggesting a balance between erosive capacity of the river and the rock-uplift pattern generated by the active fault.

[7] The 1999 Chi-Chi earthquake on the Chelungpu Fault caused intense ground motions in central Taiwan [*Dalguer et al.*, 2001]. This produced massive hillslope failures during both the earthquake and subsequent typhoons [*Dadson et al.*, 2004; *Meunier et al.*, 2007]. Thousands of these hillslope failures occurred along the Peikang River, generating a thick sediment cover that varies spatially [*Hsu et al.*, 2010]. We use this natural experiment to address the fol-

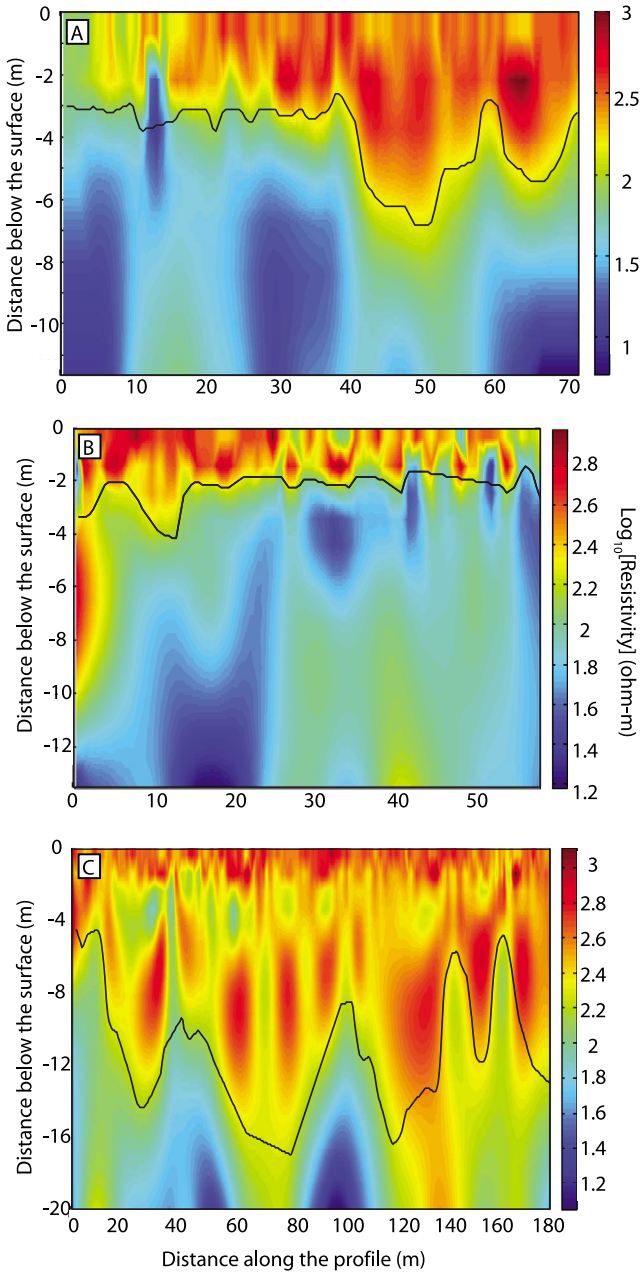


**Figure 2.** Examples of the subsurface electrical resistivity maps located along the Peikang River, central Taiwan (Figure 1) [*Hsu et al.*, 2010]. The cross section is orientated perpendicular to the flow direction of the river (looking downstream). Warm colors represent areas of high resistivity. Black line represents results of Laplacian edge detection method for finding the sediment/bedrock contact. (a) Survey 1, (b) survey 4, and (c) survey 7.

lowing questions. (1) Can streamwise variations in bed load transport capacity explain the present-day distribution of bed sediment? (2) Given that the reach is eroding bedrock over the Holocene, what inferences can we make about temporal sediment cover variability on those timescales? (3) Is there a relationship between sediment cover and incision rate? (4) Is there an appropriate field-based metric that captures the role of sediment cover? To answer these questions, we compare documented river incision rates with predictions from sediment cover models and electrical resistivity surveys, which map the depth of sediment covering bedrock in several locations along the study river. These data provide a test of proposed sediment cover models as well as reveal insight on the influence of sediment cover on bedrock river dynamics.

## 3. Methods

[8] We now describe the source of our data as well as the calculations used in our analysis. We begin by describing electrical resistivity surveys that constrain the distribution of sediment covering bedrock. Next, we introduce three sediment cover models from the literature and explain how we estimate the variables needed to calculate the frequency of bedrock exposure with each equation. We then review previous work that estimates incision rate along this river. Comparison among these data are then used to motivate a discussion focused on the role of sediment cover in controlling long-term incision rates along the Peikang River.

### 3.1. Electrical Resistivity Surveys

[9] *Hsu et al.* [2010] presented electrical resistivity surveys conducted at eight locations along the Peikang River in the spring of 2008. Seven of these locations are located near dated strath terraces that provide Holocene erosion-rate estimates [*Yanites et al.*, 2010a]. We use *Hsu et al.*'s [2010] objective Laplacian edge detection method as a guide for mapping the sediment/bedrock boundary along the channel bottom (Figure 2). This map of the subsurface contact is used to constrain the distribution of sediment depth following the Chi-Chi earthquake. The results are confirmed by a drill hole in one of the locations [*Hsu et al.*, 2010]. We only use surveys perpendicular to the flow direction and measure the depth of sediment beneath each electrode to estimate the distribution of sediment across the channel bottom. The 1 m electrode spacing of these surveys gives a vertical resolution of ~1 m [*Hsu et al.*, 2010] which we use as an estimate of our measurement error.

### 3.2. Sediment Cover

#### 3.2.1. Sediment-Cover Models

[10] Two generalized models have been proposed to calculate bedrock exposure. *Sklar and Dietrich* [2004] proposed a linear cover model

$$F = 1 - \frac{Q_S}{Q_T} \quad 0 \le Q_S \le Q_T$$
$$F = 0 \quad Q_S > Q_T, \tag{1}$$

where $F$ is the fraction of exposed bedrock, $Q_S$ is the sediment supply rate, and $Q_T$ is the sediment transport capacity. *Turowski et al.* [2007] proposed an exponential model

$$F = e^{-\varphi \frac{q_s}{q_T}} \quad 0 \le q_s \le q_t$$
$$F = 0 \quad q_s > q_t, \tag{2}$$

where $q_s = Q_s/W$, $q_T = Q_T/W$, $W$ is the width of the channel, and $\varphi$ depends on channel bed geometry and is theoretically

equal to one for a flat bed [*Turowski et al.*, 2007]. Though some data suggest that $\varphi$ may exceed one in some cases [*Turowski*, 2009], we expect that the value is still close to one. As $\varphi$ increases, significant exposure of bedrock requires increasingly greater differences between transport capacity and supply. For example, 90% bedrock exposure at $\varphi = 5$, requires capacity to exceed supply by a factor of ~50 rather than a factor of ~10 for $\varphi = 1$. Varying $\varphi$ over reasonable values does not change the trend in the results, and for simplicity, we assume $\varphi = 1$ here.

[11] A third, ad hoc model was proposed by *Lague* [2010] to explain long-term cover effects due to intermittent exposure and cover in channels subject to water and sediment discharge variability:

$$F = \exp\left(-z\left(\frac{\bar{Q}_S/\bar{Q}_T}{1-\bar{Q}_S/\bar{Q}_T}\right)^y\right), \quad (3)$$

where the bars denote average annual capacity and sediment supply. The parameters $z$ and $y$ are fitting parameters and depend on the model assumptions of *Lague* [2010]. We choose values of $z = 0.25$ and $y = 1.09$, which derive from a model run with water discharge variability on the same order as Taiwan [*Lague et al.*, 2005; *Lague*, 2010].

### 3.2.2. Sediment Supply

[12] We estimate two values of $Q_S$ for use in equations (1)–(3). The first value is simply the annual average sediment supply and is equal to

$$Q_s = \beta \rho_s E A, \quad (4)$$

where $\beta$ is the fraction of sediment in the bed load grain size fraction, $\rho_s$ is the density of rock, $A$ is the upstream contributing drainage area, and $E$ is the mean erosion rate in that area. Values of both $\beta$ and $E$ are poorly constrained for much of Taiwan. *Dadson et al.* [2003] calculated a $\beta$ of 0.30, which we adapt for consistency but note that there is a wide range of uncertainty. For the value of erosion rate, $E$, we find that an average rate 2.5 mm/yr upstream of our study area is the maximum rate allowed for $\beta = 0.30$ that satisfies the condition $Q_T > Q_S$, where $Q_T$ and $Q_S$ are the annual average sediment transport capacity and supply rate. This value is consistent with thermochronology ages for the region upstream of Reach 7 [*Dadson et al.*, 2003; *Beyssac et al.*, 2007], which supplies the majority of material for the study segment discussed here.

[13] The second value calculated is sediment supply for an individual event. This value is intended to estimate how bedrock exposure may vary along the path of the Peikang River on an individual flood timescale. Field and laboratory measurements show substantial variability in $Q_S$ for a given flood magnitude [e.g., *Singh et al.*, 2009; *Turowski et al.*, 2010]. Because data constraining bed load sediment supply and its variability for central Taiwan do not exist, we simplify our approach and assume that the annual sediment supply calculated above is transported in 10 days. We defend this assumption by noting that the bulk of the material likely moves during typhoons which strike the island ~4 times a year and last ~2.5 days each (total of 10 days) [*Wu and Kuo*, 1999]. This simplification allows an estimate of sediment supply on an event timescale that is independent of the discharge of the chosen event.

### 3.2.3. Transport Capacity

[14] We measured channel morphology with a digital elevation model and verified the measurements with field data [*Yanites et al.*, 2010a]. Channel slope was measured from a 20 m DEM and smoothed over a 1 km window to reduce inherent noise. We measured channel width perpendicular to the channel flow direction on a hillshade image of a 20 m DEM. DEM and field measurements matched well [*Yanites et al.*, 2010a]. A gauging station on the Peikang River (Figure 1) has operated for the past 35 years, providing daily discharge data over that time. Discharge at other locations was estimated by scaling linearly with drainage area upstream and downstream of the gauging station, $Q(x)/Q_G = A(x)/A_G$, where $Q(x)$ and $A(x)$ are discharge and drainage area, respectively, at point $x$, and $Q_G$ and $A_G$ are the values at the gauging station. This linear scaling is consistent with discharge data from gauging stations further downstream (http://gweb.wra.gov.tw/wrwebeng/). The channel morphology and discharge data are used to estimate the average boundary shear stress, $\tau_b$:

$$\tau_b = \rho g \left(\frac{nQ}{W}\right)^{3/5} S^{7/10}, \quad (5)$$

where $\rho$ is the density of water, $g$ is gravitational acceleration, $n$ is the Manning friction factor (assumed to equal 0.04), $W$ is channel width, and $S$ is channel slope. The average boundary shear stress is used in a Meyer-Peter-Müller bed load transport formulation [*Meyer-Peter and Müller*, 1948] to calculate transport capacity, $Q_T$ (in units of kg/s):

$$Q_T = 8\rho_s W\left[\frac{\tau_b}{(\rho_s-\rho)gD} - \tau_c^*\right]^{3/2} D^{3/2}\sqrt{\frac{(\rho_s-\rho)}{\rho}g}, \quad (6)$$

where 8 is the coefficient found by *Meyer-Peter and Müller* [1948], $\rho_s$ is the density of a sediment clast, $W$ is the width of the bed load sheet which is assumed to equal channel width in these quasi-rectangular channels, $D$ is clast grain size, and $\tau_c^*$ is the critical Shields stress for sediment entrainment and assumed to equal 0.03 (at the low end of the range identified by *Buffington and Montgomery* [1997]).

[15] We note that other formulations suggest different values for the coefficient of equation (6) [*Wong and Parker*, 2006; *Fernandez Luque and van Beek*, 1976] as well as the critical Shields stress [*Buffington and Montgomery*, 1997]; however, using these values does not change the pattern of transport capacity along the Peikang River. To remain consistent with previous work along this stretch of river [*Yanites et al.*, 2010b], we keep the original coefficient of *Meyer-Peter and Müller* [1948]. Point count measurements [*Wolman*, 1954] of 50–100 grains at 45 locations along the river provide estimates of grain size. Substantial variability of the median size did exist for individual locations (3–32 cm); however, the range of $D_{50}$ values from individual point counts within a reach is consistent from reach to reach and not correlated to transport capacity ($R^2 = 0.13$ for regression between $D_{50}$ and ten year transport capacity). For simplicity and due to the observation that surface counts tend to overestimate bulk grain size [*Mueller and Pitlick*, 2005], we assume a constant grain size of 0.1 m along stream to calculate transport capacity. We then measure annual average transport capacity

**Table 1.** Morphology, Incision Rate, and Sediment Cover Data at Each Survey Location

| Survey | Distance Downstream From Headwaters (km) | Incision Rate (mm/yr) | Annual Transport Capacity $\times 10^9$ (kg/yr) | Transport Capacity, 10 Year Flood (kg/s) | This Study, Sediment Thickness (m) | | | | Slope Change | Slope | Maximum Change in Slope (%) | *Hsu et al.* [2010], Sediment Thickness (m) | | |
|---|---|---|---|---|---|---|---|---|---|---|---|---|---|---|
| | | | | | Median Value | Min | Max | Mean | | | | Min | Max | Mean |
| L1 | 64.5 | 5.0 | 1.98 | 9660 | 3.4 | 0.9 | 6.7 | 3.6 | 0.0003 | 0.008 | | 2.4 | 6.9 | 4 |
| L21 | 61.5 | 6.5 | 3.80 | 11,133 | 3.6 | 1.2 | 9 | 4.5 | | 0.01 | 4.5 | 1.4 | 5.1 | 3 |
| L22 | 61.5 | 6.4 | 3.80 | 11,133 | 1.9 | 1.4 | 3 | 2.0 | 0.0002 | 0.01 | 0.0 | 1.3 | 5 | 3 |
| L3 | 60.2 | 8.0 | 3.82 | 10,441 | 2 | 0 | 5.7 | 2.3 | 0.0005 | 0.015 | 1.7 | 1.1 | 9.9 | 5.2 |
| L41 | 59.2 | 9.0 | 3.80 | 10,655 | 3.2 | 0 | 5 | 2.8 | −0.0015 | 0.013 | 3.7 | n/a | n/a | n/a |
| L42 | 58.6 | 9.0 | 3.92 | 11,055 | 1.9 | 0.6 | 3.3 | 1.9 | 0.0002 | 0.013 | −15.2 | 1.3 | 4.2 | 2.2 |
| L5 | 55.8 | 7.5 | 2.88 | 9304 | 2.5 | 0 | 4.8 | 2.4 | 0.0012 | 0.008 | 1.9 | 1.5 | 3.5 | 2.6 |
| L6 | 53.2 | 6.5 | 2.73 | 9781 | 4.3 | 1 | 11.4 | 5.6 | 0.0011 | 0.01 | 9.4 | 1.8 | 11.3 | 5.2 |
| L72 | 48.0 | 2.0 | 0.76 | 5487 | 11.5 | 3.6 | 15.5 | 11.1 | 0.0003 | 0.005 | 9.6 | n/a | n/a | n/a |
| L73 | 48.0 | 3.0 | 0.76 | 5487 | 10.4 | 4.3 | 12.7 | 10.4 | | 0.005 | | 9.1 | 14.5 | 12 |

by summing daily transport magnitudes and averaging over the 35 years of measurement.

[16] It is possible that channel slope may change as aggradation and sediment evacuation occur following a large earthquake, increasing the local transport capacity [*Lague*, 2010]. We test for the potential effect of this by calculating the slope change between two reaches by differencing the mean sediment thicknesses in the two reaches and then dividing by the horizontal distance between the reaches. This leads to an estimate of the percent change in slope (Table 1). Also, the rectangular shape and bedrock walls of the Peikang River limit channel width; therefore, the addition of alluvial cover will not immediately affect channel width.

[17] We also find it is informative to calculate the transport capacity differences along the Peikang for a single flood event and choose the 10 year discharge as a representative flood. Records from gauging station H01430, located at ~55 km downstream from the headwaters (Figure 1), eveal that this discharge is ~1000 $m^3/s$. Choosing the 10 year discharge provides a measure of relative sediment cover variability along the Peikang River for a flow that is well beyond the critical discharge for entrainment for all reaches. This value is simply meant to give an estimate of sediment transport capacity (and sediment cover) differences during a single flood event.

### 3.3. Incision Rate

[18] Optically stimulated luminescence (OSL) dating of fluvial deposits on bedrock strath terraces provides estimates of incision rates [*Yanites et al.*, 2010a]. Because the deposits are fluvial in origin with no postdepositional disturbance, the OSL dates give a maximum age of terrace abandonment. Elevation differences between the bedrock level of the abandoned terrace and the bedrock level of the modern river constrain the depth of incision since the time of abandonment. Samples were collected and processed following standard single-aliquot regenerative-dose procedures [*Murray and Wintle*, 2000]. Statistical analysis of the aliquot data supports the use of a minimum-age model for all samples in determining deposition age [cf. *Arnold et al.*, 2007]. This age model is commonly applied to fluvial sediments in order to account for the likelihood of partial bleaching [*Wallinga*, 2002]. The standard deviations of the aliquot data as well as uncertainty in the depth of incision are used to estimate error bounds. Details of the strath-terrace dating reported by *Yanites et al.* [2010a] reveal a few Late Pleistocene and mostly Holocene ages for terraces along this reach.

## 4. Results

[19] For each electrical resistivity survey, we calculate the local transport capacity and sediment supply (Figure 3a). Not all survey locations are near an estimate for local incision rate, so we interpolate between OSL locations to obtain an estimate of Holocene incision rate at each survey position (Figure 3c). Errors are calculated by averaging the percent error of nearby (within 5 km) incision rate estimates. Reaches 2 and 7 had repeat surveys within 100 m of each other to check for consistency. To ensure that these survey points are discernable in Figures 3c, 6, and 7, we assign slightly different incision rates for the adjacent surveys (Table 1) but within the range of local estimates of erosion rates.

[20] The depth of sediment varies spatially along the Peikang River (Figure 3b and Table 1). The trend in the depth of sediment mirrors the trends in incision rate, which appears to be dictated by the active Shuilikeng fault [*Yanites et al.*, 2010a], and transport capacity (Figures 3 and 4). For example, maximum sediment depth occurs in reach 7 (surveys 7-1 and 7-2), which also has the lowest Holocene incision rate (~1–2 mm/yr) and low transport capacity (Figure 3). Minimal sediment depth occurs in reaches 3 and 4, where there is a high rate of Holocene incision as well as high transport capacity. The range (max and min) of our interpreted results is slightly different from the analysis of *Hsu et al.* [2010] although the trend is similar (Table 1). The reason for the discrepancy is that we ignored the depths within 5 m of the survey edge to be sure we were not incorporating inversion edge effects into our distributions.

[21] River cross-section data from the Water Resource Agency of Taiwan reveal significant aggradation following the 1999 Chi-Chi earthquake at gauging station 1430H032 (Figure 5) (http://gweb.wra.gov.tw/wrwebeng/). Following the 1999 earthquake, ~3.5 m of sediment had aggraded in this reach as of 2005, clearly indicating that sediment supply, $Q_S$, outpaced transport capacity, $Q_T$, following the earthquake. This value is close to the median value of

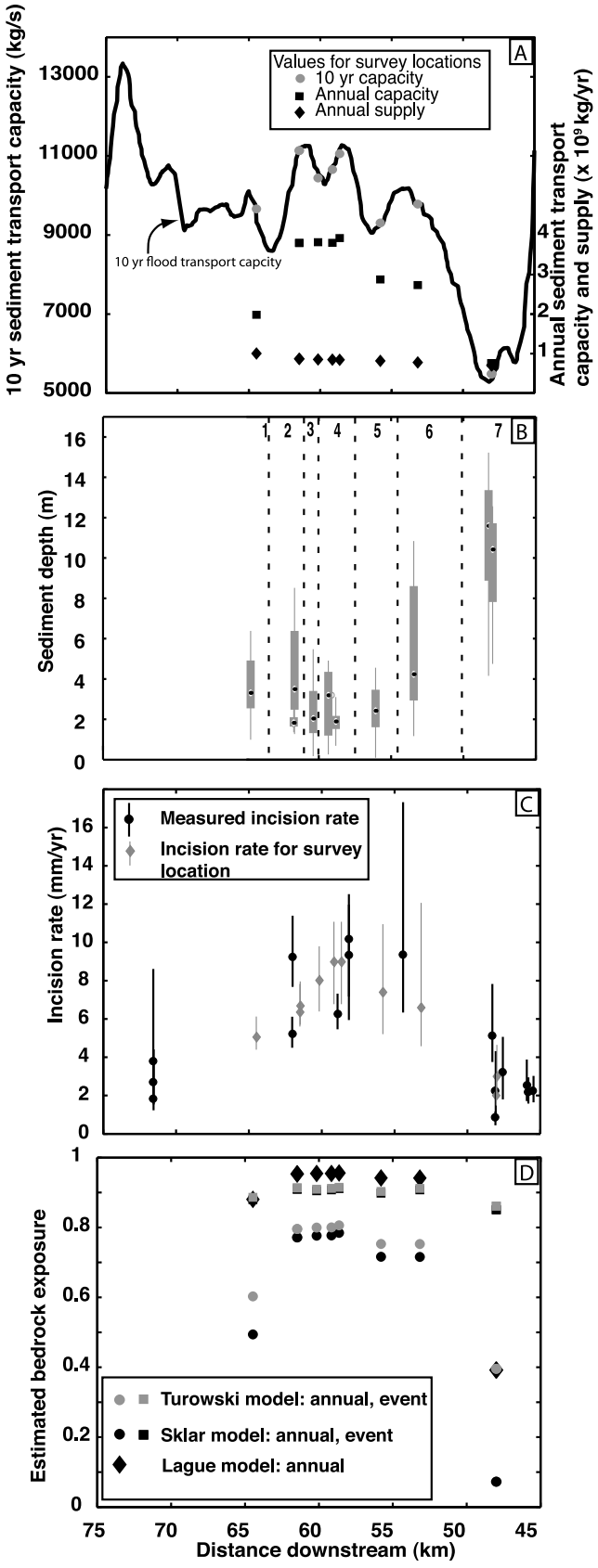


**Figure 3.** (a) Transport capacity, (b) sediment depth, (c) incision rate estimated with OSL dating of fluvial sediments on strath terraces, and (d) bedrock exposure along the Peikang River. Transport capacity is reported for both annual estimates at each resistivity survey as well as the 10 year flood capacity along the flow path. Also plotted is the estimated annual sediment supply calculated by assuming an average upstream erosion rate and the proportion of that material transported by bed load (see text for details). Sediment depth is plotted in box and whisker form. Dashed lines denote the boundaries for the numbered reaches. Bedrock exposure for all estimated sediment cover models is presented.

sediment cover of the nearby resistivity Survey 5 (2.5 m), ~600 m upstream.

[22] Bedrock exposure is predicted to vary spatially along the path of the Peikang River (Figure 3). For all proposed bedrock exposure models, the pattern reflects the spatial variation in incision rate, transport capacity, and measured sediment depth, with maximum bedrock exposure where incision rate is highest and minimum where incision is low (Figure 6). The specific values are highly variable and dependent on assumptions used to calculate sediment supply and transport capacity. Nonetheless, as long as the constraint that $Q_T > Q_S$ is valid, the trend in Figure 6 will remain robust.

[23] It is worth noting the difference in the along-stream range of bedrock exposure values between the annual and event-based estimates (Figure 6). This results from the annual estimates incorporating events in which the threshold of motion is exceeded in some reaches but not in all. Essentially, relatively small discharge events can entrain bed load (and potentially expose bedrock to erosion) in the high capacity reaches whereas the low capacity reaches remain below the sediment transport threshold and thus have a transport capacity of zero. Because of the differences in the frequencies of transport events, averaging over the full distribution of discharges produces a wider range in the relative sediment transport capacities than a single event.

## 5. Discussion

[24] The most important result of this study is the correlation among measured sediment depth, estimated bedrock exposure, and incision rate (Figures 4 and 6). We argue that this correlation reflects the importance of sediment cover variability in controlling long-term incision rates along the Peikang River, central Taiwan. Essentially, the spatial distribution of sediment depth reveals the role of sediment cover in modulating the frequency of active bedrock incision events along the study reach of the Peikang River. As such, we propose that the median sediment thickness may provide a valid proxy for the long-term relative influence of sediment cover on erosion rates along bedrock rivers. We stress our use of the term 'relative' here to highlight the extreme difficulty of ever knowing the true value of bedrock exposure in systems subject to high variability in both water and sediment discharge [*Lague*, 2010; *Johnson et al.*, 2010]. In fact, our observations here constrain the magnitude of sediment covering bedrock for only one point in time, and

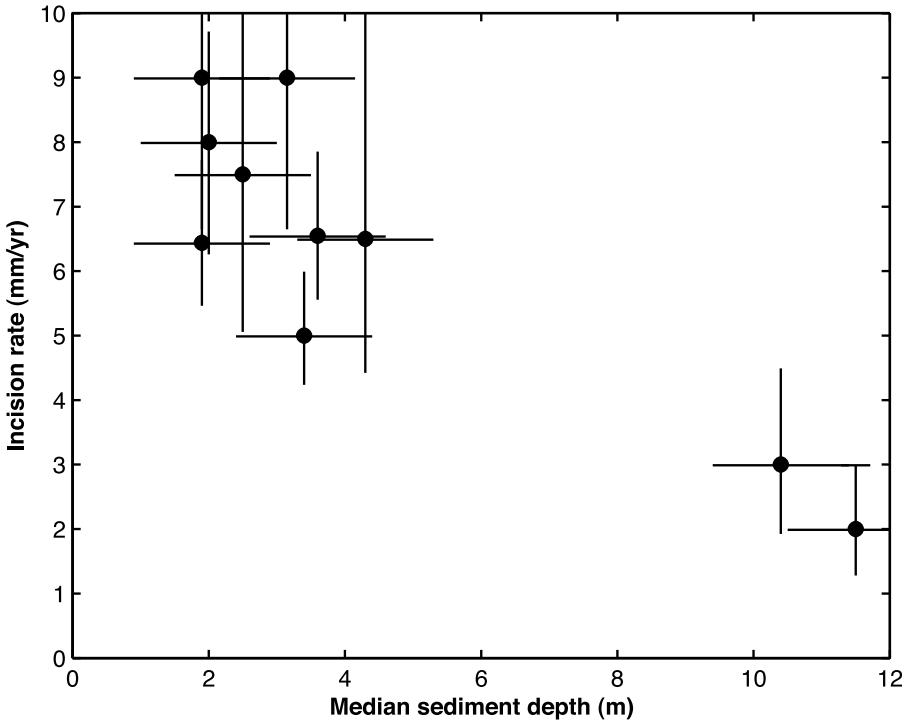


**Figure 4.** Median sediment depth versus incision rate.

we do not know the distribution of sediment thickness prior to the Chi-Chi earthquake. Nonetheless, there are many reasons discussed below that support the notion that sediment cover is important along the Peikang River and that sediment depth may serve as a proxy for the relative influence along the river. The following discussion is aimed at backing these claims.

### 5.1. Role of Sediment Cover in Long-Term Incision Rate and Morphology

[25] The correlations between incision rate, sediment depth, and calculated exposure fraction ($F$) raise the question of whether $F$ is the primary control on long-term incision, or is merely a second-order effect (Figure 6). One can envision four general possibilities, each of which offers some basic predictions that can be addressed with data from the Peikang River.

[26] Scenario 1 is that all the reaches have the same degree of bedrock exposure, and differential incision is entirely due to variations in erosion potential (as indicated by a proxy such as unit stream power). This predicts that erosion potential should correlate with incision rate but bedrock exposure should not vary along the Peikang. Unit stream power does correlate with incision rate [*Yanites et al.*, 2010a], but this correlation is strongly controlled by variations in channel width, rather than channel slope. Such a relationship is inconsistent with a river where bedrock exposure is not important [*Turowski et al.* [2007]; *Yanites and Tucker*, 2010]. Using a channel geometry optimization model that accounts for the effects of sediment cover, *Yanites and Tucker* [2010] predict that the dominant morphological adjustment of a channel (i.e., a change in width or a change in slope) to different erosion rates depends on the degree of bedrock exposure. When bedrock exposure is high and sediment cover is insignificant, channel slope increases more than the channel narrows in response to greater incision rates. Conversely, when bedrock exposure is low and sediment cover is significant, increases in erosion are accomplished primarily through channel narrowing rather than steepening. Further, bedrock exposure is clearly not uniform along the Peikang River and is indeed correlated

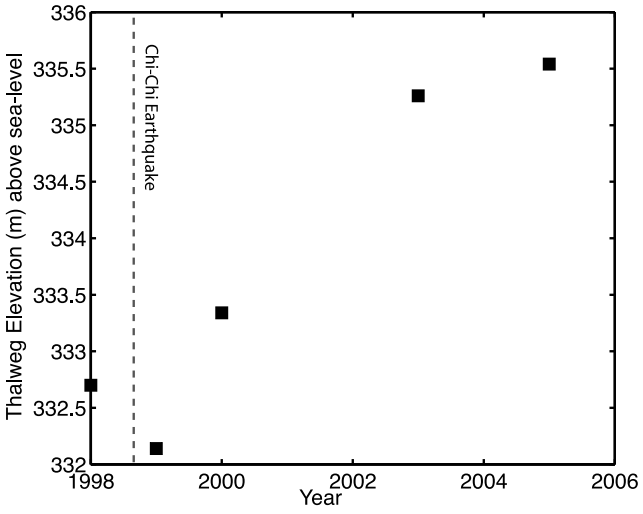


**Figure 5.** Elevation of the thalweg at gauging station 1430H032 over an 8 year period. Data taken from the minimum elevation of cross sections measured by the Water Resource Agency of Taiwan. Dashed line represents time of the $M_w$ = 7.6 Chi-Chi earthquake.

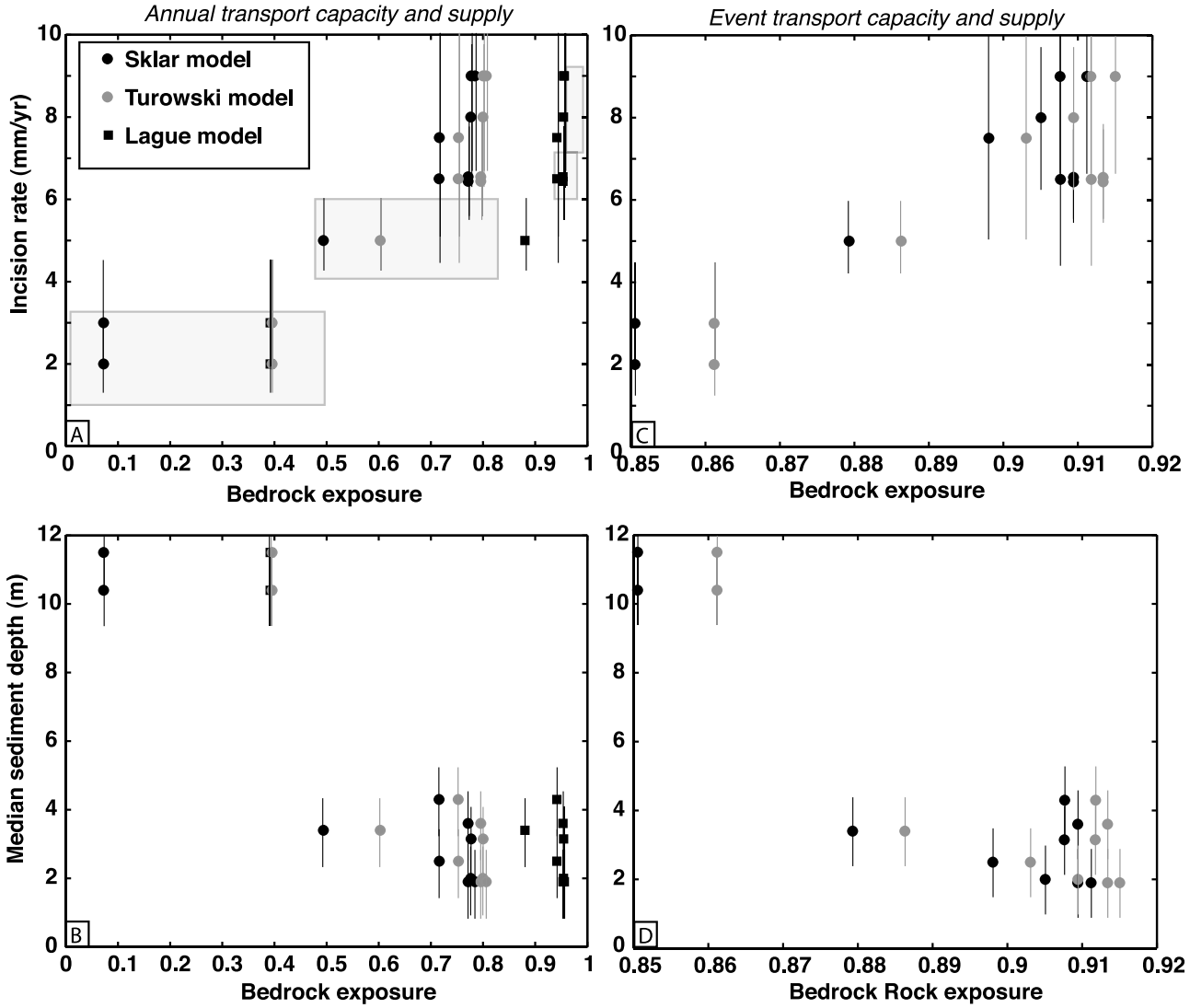


**Figure 6.** Incision rate and sediment depth versus bedrock exposure. (a) Incision rate versus bedrock exposure estimates calculated using annual average transport capacity and supply. Boxes denote estimates of bedrock exposure calculated from reach scale estimates of landslide material evacuation times following the Chi-Chi earthquake. Box ranges along the incision axis reflect the variation of incision rates in that reach. Width along the *x* axis reflects uncertainty in the volume of landslide material released by the earthquake. See text for explanation. (b) Median sediment depth versus bedrock exposure using the same values as in Figure 6a. (c) Incision rate versus bedrock exposure estimates using 10 year flood transport capacity and an estimate of event based sediment supply. (d) Median sediment depth versus bedrock exposure estimates from Figure 6c.

with incision rate. Thus, unless today's cover patterns are a momentary aberration, this possibility can be ruled out.

[27] Scenario 2 is that incision rate is solely determined by the degree of bedrock exposure. In this scenario, one might predict that all reaches have either the same unit stream power or that unit stream power is uncorrelated with incision rate. Unit stream power is not uniform along the Peikang River and is strongly correlated with incision rate [*Yanites et al.*, 2010a]; however, we cannot rule out that the correlation between unit stream power and incision rate simply reflects the relative transport capacity in these reaches. Therefore, we cannot determine the degree to which hydraulics, serving as a proxy for the intensity of erosive processes during periods of bedrock exposure, matter or not.

[28] Scenario 3 is that the system is transport-limited. In such a system, when sediment supply from upstream is less than the transport capacity for a given reach, the river incises bedrock to add transportable material at a rate such that the river transports sediment at its full capacity. This implies that bedrock incision processes are not at all important and the rate of incision is dictated by the divergence of sediment transport capacity in the downstream direction. If this were the case, the magnitude of this divergence should match the incision rate. The divergence of transport capacity, however, is not reflective of the incision rate (Figure 3a). For example,

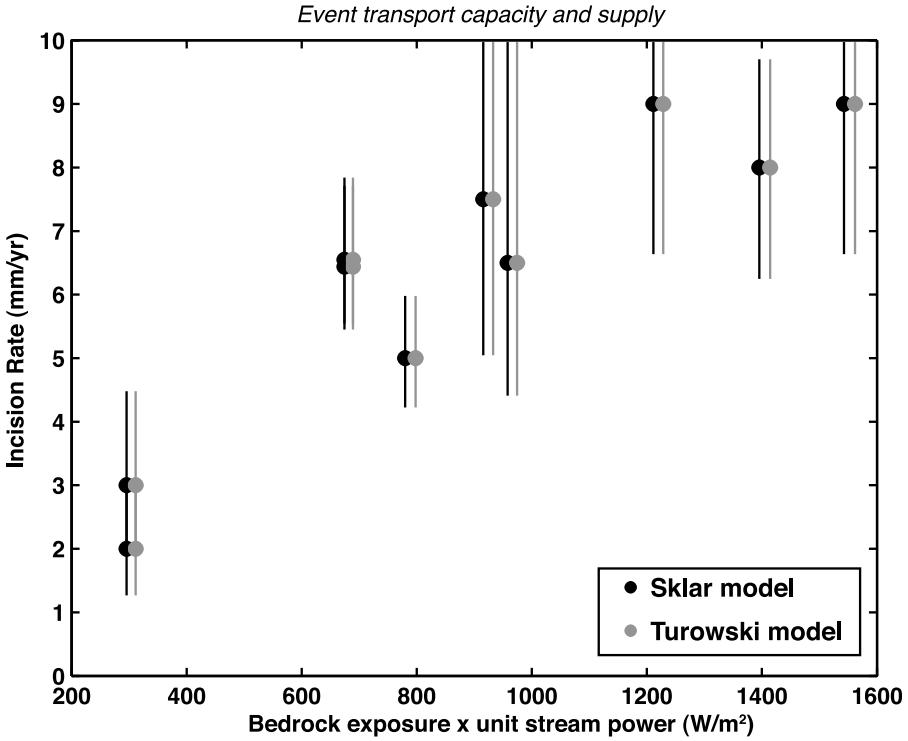


**Figure 7.** Incision rate versus the product of bedrock exposure and stream power. Bedrock exposure and stream power are estimated using the 10 year flood event.

the transport capacity between 45 and 50 km downstream in Reach 7 has a negative divergence and should be undergoing long-term aggradation rather than incision. Because Reach 7 is incising and transport capacity decreases in the downstream direction, we can firmly say that river erosion along the Peikang is not limited by transport capacity. Therefore, scenario 3 can be ruled out.

[29] Scenario 4 is that incision rate depends on both bedrock exposure and unit stream power (as a proxy for incision intensity). This predicts that both bedrock exposure and unit stream power correlate with incision rate. Further, the product of these parameters should strongly correlate with the incision rate. This is well supported by data along the Peikang River for an event timescale (Figure 7). From Figure 7, it could be argued that incision rate and the product of stream power and bedrock exposure are linearly related. We avoid calculating this for the annual transport capacity/supply bedrock exposure functions since it would require extra assumptions about the relationship between sediment supply and discharge for each measure of daily discharge over the past 35 years; however, given the similarities in trends between the annual and 10 year estimates of bedrock exposure (Figures 3 and 6), a similar trend would likely result if the sediment supply distribution were known. *Lague* [2010] simulated this scenario by assuming a functional relationship between sediment supply and discharge. We cannot directly compare our results with his work since he did not calculate a scenario with different erosion rates along a flow path; however, he did find that by varying rock-uplift rate in different simulations, there was a relationship between incision rate and sediment cover. Interestingly, he found that increasing rock-uplift rate by an order of magnitude did not change the sediment regime by the same magnitude, suggesting that increases in both bedrock exposure and erosion potential were important. Although modeling bedrock channel geometries in a scenario similar to the Peikang River (i.e., differential rock-uplift rate) is beyond the scope of this paper, it is likely that the conclusions would be similar, that is both bedrock exposure and erosion intensity are important in controlling long-term erosion rates.

[30] Scenarios 2 and 4 both explain the incision rate variability along the Peikang River. Although we cannot distinguish between these scenarios, both require that exposure of bedrock to fluvial incision processes fundamentally controls long-term incision rates. The relative importance of the intensity of erosive processes on exposed bedrock, however, is uncertain. It remains possible, although unlikely, that the relative erosive 'intensities' measured by unit stream power and shear stress do not influence long-term incision and that the correlation measured [*Yanites et al.*, 2010a] merely reflects the transport capacity's control on bedrock exposure. Another important observation along that Peikang River is that channel width is strongly anticorrelated with erosion rate yet slope is only slightly correlated [*Yanites et al.*, 2010a]. *Yanites and Tucker* [2010] predict that such a relationship is likely for rivers carrying significant bed load and having bedrock exposures between ~0.1 and ~0.9. For these reasons, we suggest scenario 4 best describes the Peikang River.

### 5.2. Temporal Variability in Sediment Cover

[31] The balance between sediment supply and transport determines whether bed aggradation or exposure occurs. The average depth of sediment along a river reach at any

point in time, $h(t)$, is ultimately controlled by the rate of sediment supplied to the reach, $Q_S$, and the rate at which sediment is transported out of the reach, $Q_T$:

$$h(t) = h_0 + \int_0^T \frac{Q_S(t) - Q_T(t)}{A(t)} dt, \quad (7)$$

where $A(t)$ is the product of channel width and reach length, $h_0$ is the initial depth of sediment (at $t = 0$), and $T$ is some time in the past over which the chosen values for $Q_T$ and $Q_S$ are appropriate. There exists the potential for a feedback as changes in $h$ can change bed slope and therefore increase $Q_T$ [*Lague*, 2010]. Given the measured along stream differences in $h$ (max 10m) and the distance between the surveys (2–5 km), it is clear that potential slope and transport capacity changes are small compared to current values (Table 1). Also, because of the rectangular cross section of the Peikang River, changes in $h$ do not affect channel width or $A$. Thus, along the Peikang River, bedrock morphology controls the river transport capacity, and it does not change drastically due to perturbations in $Q_S$.

[32] As indicated by the temporal changes in thalweg depth at the gauging station, sediment depth is not steady along the Peikang River though the recent leveling off of aggradation suggests that supply and capacity are now close to balanced as the river system evacuates the pulse of sediment coming from the hillslopes (Figures 1 and 5). For this system, any increases in $Q_T$ due to slope changes from aggradation are outpaced by increases in $Q_S$ from the pulse of landslide material. At some point in the future, $Q_S$ will decrease as the rivers have evacuated the pulse of landslide material, and $h(t)$ will decrease, increasing bedrock exposure.

[33] The sediment cover in Reach 7 further supports the assertion that sediment cover varies temporally. Because on the order of 10 m of sediment overlie bedrock, we can safely assume that no vertical bedrock incision is taking place at present; however, reach 7 is eroding at 1–2 mm/yr over Holocene timescales (Figure 3b). Sediment cover must vary temporally to maintain this long-term rate of incision. Additionally, when bedrock is uncovered and exposed, erosion rates must exceed 1–2 mm/yr in order to incise at the long-term rate. To expose bedrock underlying the sediment cover in Reach 7, either one or both of the following scenarios must occur: (1) the reach must increase transport capacity through either significantly changing channel morphology or increasing water discharge, or (2) sediment supply must decrease. For the former situation, substantial changes in channel morphology would take a significantly long time to accomplish since it requires bedrock erosion (Table 1). For example, given incision rate gradient magnitudes on the order of 1mm/yr per river kilometer, it would take 1000 years to change the modern river slope by 0.001, or about 10% of its current value (Figure 3c). Increased water discharge, from events such as extraordinarily large typhoons or an increase in typhoon frequency, would likely significantly increase sediment supply due to mass movements on the hillslopes. A reduction in sediment supply to these reaches, however, is a plausible scenario as the river basin removes the material released by landslides during and just after the Chi-Chi earthquake. The 1999 Chi-Chi earthquake and subsequent typhoons cleared a substantial amount of mass from hillslopes [*Meunier et al.*, 2007] compared to the long-term erosion rate. A significant fraction of this mass is likely too coarse to be transported in suspension [e.g., *Lin et al.*, 2008] and will thus be evacuated by bed load transport. Estimates of the evacuation rate of the coarse grain-size fraction of the landslide material suggest decade to century timescales to remove this earthquake-generated pulse of sediment [*Yanites et al.*, 2010b]. After the removal of the bed load size fraction, the reduction in sediment supply should result in less sediment cover and an increase in bedrock erosion.

[34] Using the calculated values of evacuation time from *Yanites et al.* [2010b] along with an estimate of ~500 years for the recurrence interval of a Chi-Chi type earthquake from paleoseismic data [*Chen et al.*, 2004], we can constrain a temporally averaged long-term bedrock exposure fraction along the Peikang River. We assume the end-member scenario of full cover during evacuation and full bedrock exposure after evacuation. Uncertainty in total landslide volume generates a range of evacuation times for each reach [*Yanites et al.*, 2010b] and therefore a range of estimates of bedrock exposure. We plot these estimates with the range of incision rates in each reach of *Yanites et al.* [2010b] in Figure 6. Note that this is likely an overestimate since after evacuation, bedrock exposure is likely less than 100%. Nonetheless, the results of this simple exercise are interesting and are consistent with estimates of $F$ using annual transport capacity and supply values. The differences in temporal controls on bedrock exposure along the Peikang River are correlated with incision rate, suggesting that incision is modulated by sediment cover variability along the Peikang River.

[35] A few simple calculations can reveal the importance of temporal variability along the river. For example, if reach 7 takes 400 years to evacuate the landslide material and is eroding at 1 mm/yr over the Holocene, then the river must incise at 5 mm/yr during the 100 years of exposure prior to the next earthquake. On the other hand, reach 4 is only buried for ~20 years, so that when exposed, erosion rates are only slightly exaggerated beyond long-term averages, though still higher than expected instantaneous rates in reach 7. We note that these estimates of instantaneous rates are comparable to other bedrock rivers in Taiwan over various timescales [*Dadson et al.*, 2003; *Schaller et al.*, 2005; *Hartshorn et al.* 2002; *Turowski et al.*, 2008a; *Stock et al.*, 2005]. Thus although there is an approximately fivefold difference in long-term incision rates between reaches 4 and 7, the difference between instantaneous erosion rates when erosion is occurring in these reaches is less than twofold. Thus the changes in erosion rates along the Peikang River must be strongly influenced by differences in temporal sediment cover.

### 5.3. Spatial Variability in Sediment Cover

[36] The clear dependency of incision rate on sediment cover along the Peikang River offers a chance to analyze field-based metrics that document the role of sediment cover on long-term incision rates. Numerical modeling [*Lague*, 2010] predicts that variability in sediment supply and discharge causes temporal variability in the degree of cover in a bedrock river. Because sediment cover is ultimately tied to the differences between supply and transport (equation (7)),

we suggest that in cases such as the Peikang River, where capacity and incision vary systematically downstream, a measure of the thickness of material in a cross section of the river will document the relative role of sediment cover along the river path. This hypothesis implies that if sediment cover is important in controlling long-term river erosion, then sediment thickness along the river path will reflect this [e.g., *Lague*, 2010]; however, if sediment cover is not important, and only the intensity of erosive processes control erosion rates, then there will be no measurable correlation among sediment cover, sediment depth, and incision rate. In these later cases, the river transport capacity greatly outpaces supply along the entire flow path, and the river could thus be described as erosion potential limited.

[37] Clearly the modern sediment cover following the Chi-Chi earthquake is not constant over time; however, our hypothesis suggests that the spatial distribution of modern sediment covering bedrock serves as a proxy for the relative long-term sediment cover distribution along the river. This is rooted in the idea that smaller hillslope events (relative to the Chi-Chi driven landslides) likely produce a spatially similar but smaller-in-magnitude distribution of sediment depth along the river. In this hypothesis, we assume that the events responsible for delivering the bulk of sediment to the main stem river (i.e., typhoons and earthquakes), operate over sufficiently large spatial scales that this stretch of river receives relatively uniform 'punches' of sediment delivery, since the tributaries integrate and 'smooth' the variability caused by individual landslides. We note that spatial variability will exist within an individual tributary, where the bulk of the material is generated, but as evidenced by the sedimentation rate at the gauging station (Figure 4), we suspect that this variability will smooth out in a matter of years as the material transits the tributary. In other words, this idea suggests that reaches with a relatively thick sediment mantle today also tended to have thicker and/or more frequent sediment cover in the geologic past (and vice versa). Essentially, Reaches 3 and 4 have had the least sediment cover (and greatest bedrock exposure) over the Holocene, whereas Reach 7 has the greatest (Figures 3 and 6). The logic for this assumption lies in the conservation of mass along a river (equation (7)). Because the relative differences between $Q_S$ and $Q_T$ from reach to reach will remain the same along the Peikang River over time, the sediment depth, $h$, reflects the relative differences between these variables and therefore should serve as a proxy for $F$. This is reflected in the data. Figure 6 shows that reaches with thin cover today (e.g., reaches 3 and 4) are expected to have the greatest frequency of bedrock exposure both with an individual flood (Figures 3 and 6b) and over the long-term (Figures 3 and 6a), whereas reaches with thick cover (reach 7) have the least exposure of bedrock. This supports our hypothesis and provides evidence that sediment depth is indeed serving as a proxy for long-term sediment cover.

[38] River incision along the Peikang River is spatially and temporally variable. This finding is not in itself very surprising; however the reason for the incision-rate variability is interesting. It is variable not necessarily because of variation in water discharge, although that will introduce temporal variability on daily to annual scales, but rather because of the fluctuations in sediment cover [e.g., *Lague*, 2010]. The magnitude of sediment cover is variable is both space and time and is controlled locally and temporally by the relative magnitudes of sediment supplied from the hillslopes and transport capacity.

[39] Spatial variability in sediment cover is likely to exist in a given flood (Figures 3 and 6); however, we contend that the temporal variability is a stronger control on long-term incision rates. The reason for this is that the range of timescales of response to a given 'kick' in sediment supply is rather large along the path of the river. For example, *Yanites et al.* [2010b] calculate an order of magnitude difference in evacuation of landslide material following the Chi-Chi earthquake, whereas the spatial variation of a given event, calculated in this study, is rather small (Figure 6). Nonetheless, it is clear that some manifestation of $Q_S/Q_T$ captures bedrock exposure since the ratio will control the response time to sediment supply perturbations.

[40] Finally, because sediment transport capacity is set by the channel morphology (slope and width), it is not likely to change very rapidly with time and is therefore more reflective of long-term forcings. Modern sediment cover is clearly not steady and reflects the annual to decadal seismic and meteorological history of the basin. This brings up an important point in that channel morphology is reflective of the long-term integrated effects of base level fall and sediment supply, whereas the current bed state (i.e., sediment cover/depth) depends highly on the stochastic nature of recent events including both sediment supply and water discharge. Continued monitoring and measuring of the distribution of sediment along the Peikang River and other bedrock rivers will help illuminate the importance of spatial and temporal variability of sediment cover in these systems.

## 6. Summary and Conclusions

[41] The distribution of sediment depths along the Peikang River following the 1999 Chi-Chi earthquake implies that sediment cover frequency can control long-term incision rates. In the low transport capacity reaches vertical bedrock incision has stopped, and in the relatively high-capacity reaches, sediment cover has slowed incision. Reaches with higher transport capacity buffer erosion by sediment cover less than other reaches and erode at higher long-term rates. Because the low-capacity reaches incise bedrock over Holocene timescales, our results require temporal variations in sediment cover. Records from a gauging station that show ~3.4 m of aggradation following the Chi-Chi earthquake further support significant temporal variation in sediment cover. The morphology of a bedrock river fed by a temporally and spatially varying sediment supply is set to both incise at the rate of base level fall (with respect to downstream) and eventually transport all sediment supplied to it. As a river deals with different sediment loads throughout its history, it undergoes different instantaneous erosion rates; however, the local transport capacity, controlled by the width and slope, is set such that the long-term integrated incision rate matches the local rock-uplift rate.

[42] Though spatial variability in bedrock exposure likely exists during individual flood events, we find that it is the temporal response of sediment cover to large fluxes of sediment that dominates along the Peikang River in central Taiwan. Further, the depth of sediment along the Peikang River correlates with model predictions of exposure. We

suggest that the median sediment depth along the flow path is a potential field metric that serves as a proxy for the long-term role of sediment cover in controlling incision rates. Considering the data presented here, we conclude that sediment cover strongly modulates incision rates along the Peikang River.

[43] **Acknowledgments.** Funding was provided by NSF grant EAR-0510971 to K.M. and G.T., NSF grant EASPI-0611725 to B.Y., and a NDSEG fellowship to B.Y. The manuscript benefited from thorough and constructive reviews by Mikaël Attal, Jens Turowski, Dimitri Lague, and the Associate Editor.

## References

Arnold, L. J., R. M. Bailey, and G. E. Tucker (2007), Statistical treatment of fluvial dose distributions from southern Colorado arroyo deposits, *Quat. Geochronol.*, *2*, 162–167, doi:10.1016/j.quageo.2006.05.003.

Benda, L., and T. Dunne (1997), Stochastic forcing of sediment supply to channel networks from landsliding and debris flow, *Water Resour. Res.*, *33*, 2849–2863, doi:10.1029/97WR02388.

Beyssac, O., M. Simoes, J. P. Avouac, K. A. Farley, Y. G. Chen, Y. C. Chan, and B. Goffe (2007), Late Cenozoic metamorphic evolution and exhumation of Taiwan, *Tectonics*, *26*, TC6001, doi:10.1029/2006TC002064.

Buffington, J. M., and D. R. Montgomery (1997), A systematic analysis of eight decades of incipient motion studies, with special reference to gravel-bedded rivers, *Water Resour. Res.*, *33*, 1993–2029, doi:10.1029/96WR03190.

Bull, W. B. (1979), Threshold of critical power in streams, *Geol. Soc. Am. Bull.*, *90*, 453–464, doi:10.1130/0016-7606(1979)90<453:TOCPIS>2.0.CO;2.

Chatanantavet, P., and G. Parker (2008), Experimental study of bedrock channel alluviation under varied sediment supply and hydraulic conditions, *Water Resour. Res.*, *44*, W12446, doi:10.1029/2007WR006581.

Chen, W. S., K. J. Lee, L. S. Lee, D. J. Ponti, C. Prentice, Y. G. Chen, H. C. Chang, and Y. H. Lee (2004), Paleoseismology of the Chelungpu Fault during the past 1900 years, *Quat. Int.*, *115–116*, 167–176, doi:10.1016/S1040-6182(03)00105-8.

Cowie, P. A., A. C. Whittaker, M. Attal, G. Roberts, G. E. Tucker, and A. Ganas (2008), New constraints on sediment-flux–dependent river incision: Implications for extracting tectonic signals from river profiles, *Geology*, *36*, 535–538, doi:10.1130/G24681A.1.

Dadson, S. J., et al. (2003), Links between erosion, runoff variability and seismicity in the Taiwan orogen, *Nature*, *426*, 648–651, doi:10.1038/nature02150.

Dadson, S. J., et al. (2004), Earthquake-triggered increase in sediment delivery from an active mountain belt, *Geology*, *32*, 733–736, doi:10.1130/G20639.1.

Dalguer, L. A., K. Irikura, J. D. Riera, and H. C. Chiu (2001), The importance of the dynamic source effects on strong ground motion during the 1999 Chi-Chi, Taiwan, earthquake, Brief interpretation of the damage distribution on buildings, *Bull. Seismol. Soc. Am.*, *91*, 1112–1127, doi:10.1785/0120000705.

Fernandez Luque, R., and R. van Beek (1976), Erosion and transport of bed-load sediment, *J. Hydraul. Res.*, *14*, 127–144, doi:10.1080/00221687609499677.

Finnegan, N. J., L. S. Sklar, and T. K. Fuller (2007), Interplay of sediment supply, river incision, and channel morphology revealed by the transient evolution of an experimental bedrock channel, *J. Geophys. Res.*, *112*, F03S11, doi:10.1029/2006JF000569.

Finnegan, N. J., B. Hallet, D. R. Montgomery, P. K. Zeitler, J. O. Stone, A. M. Anders, and L. Yuping (2008), Coupling of rock uplift and river incision in the Namche Barwa–Gyala Peri massif, Tibet, *Geol. Soc. Am. Bull.*, *120*, 142–155, doi:10.1130/B26224.1.

Gilbert, G. K. (1877), *Report on the Geology of the Henry Mountains*, 160 pp., U.S. Gov. Print. Off., Washington, D. C.

Hartshorn, K., N. Hovius, W. B. Dade, and R. L. Slingerland (2002), Climate-driven bedrock incision in an active mountain belt, *Science*, *297*, 2036–2038, doi:10.1126/science.1075078.

Hsu, H. L., B. J. Yanites, C. C. Chen, and Y. G. Chen (2010), Bedrock detection using 2D electrical resistivity imaging along the Peikang River, central Taiwan, *Geomorphology*, *114*, 406–414, doi:10.1016/j.geomorph.2009.08.004.

Johnson, J. P., and K. X. Whipple (2007), Feedbacks between erosion and sediment transport in experimental bedrock channels, *Earth Surf. Processes Landforms*, *32*, 1048–1062, doi:10.1002/esp.1471.

Johnson, J. P. L., and K. X. Whipple (2010), Evaluating the controls of shear stress, sediment supply, alluvial cover, and channel morphology on experimental bedrock incision rate, *J. Geophys. Res.*, *115*, F02018, doi:10.1029/2009JF001335.

Johnson, J. P., K. X. Whipple, L. S. Sklar, and T. C. Hanks (2009), Transport slopes, sediment cover, and bedrock channel incision in the Henry Mountains, Utah, *J. Geophys. Res.*, *114*, F02014, doi:10.1029/2007JF000862.

Johnson, J. P., K. X. Whipple, and L. S. Sklar (2010), Contrasting bedrock incision rates from snowmelt and flash floods in the Henry Mountains, Utah, *Geol. Soc. Am. Bull.*, *122*, 1600–1615, doi:10.1130/B30126.1.

Korup, O., and D. R. Montgomery (2008), Tibetan plateau river incision inhibited by glacial stabilization of the Tsangpo gorge, *Nature*, *455*, 786–789, doi:10.1038/nature07322.

Lague, D. (2010), Reduction of long-term bedrock incision efficiency by short-term alluvial cover intermittency, *J. Geophys. Res.*, *115*, F02011, doi:10.1029/2008JF001210.

Lague, D., N. Hovius, and P. Davy (2005), Discharge, discharge variability, and the bedrock channel profile, *J. Geophys. Res.*, *110*, F04006, doi:10.1029/2004JF000259.

Lamb, M. P., W. E. Dietrich, and L. S. Sklar (2008), A model for fluvial bedrock incision by impacting suspended and bed load sediment, *J. Geophys. Res.*, *113*, F03025, doi:10.1029/2007JF000915.

Lin, G. W., et al. (2008), Effects of earthquake and cyclone sequencing on landsliding and fluvial sediment transfer in a mountain catchment, *Earth Surf. Processes Landforms*, *33*, 1354–1373, doi:10.1002/esp.1716.

Meunier, P., N. Hovius, and A. J. Haines (2007), Regional patterns of earthquake-triggered landslides and their relation to ground motion, *Geophys. Res. Lett.*, *34*, L20408, doi:10.1029/2007GL031337.

Meyer-Peter, E., and R. Müller (1948), Formulas for bed-load transport, *Proceedings of the 2nd Meeting of the International Association of Hydraulic Structures Research*, *Stockholm, Sweden*, pp. 39–64, Int. Assoc. Hydraul. Res., Delft, Netherlands.

Mueller, E. R., and J. Pitlick (2005), Morphologically based model of bed load transport capacity in a headwater stream, *J. Geophys. Res.*, *110*, F02016, doi:10.1029/2003JF000117.

Murray, A. S., and A. G. Wintle (2000), Luminescence dating of quartz using an improved single-aliquot regenerative-dose protocol, *Radiat. Meas.*, *32*, 57–73, doi:10.1016/S1350-4487(99)00253-X.

Powell, L. K. (2003), Feedback between erosion and fault reactivation in the Puli Basin: Hsuehshan Belt of Central Taiwan, M.S. thesis, Dep. of Geol. Sci., Univ. of Colo. at Boulder, Boulder.

Schaller, M., N. Hovius, S. D. Willet, S. Ivy-Ochs, H. A. Synal, and M. C. Chen (2005), Fluvial bedrock incision in the active mountain belt of Taiwan from in situ-produced cosmogenic nuclides, *Earth Surf. Processes Landforms*, *30*, 955–971, doi:10.1002/esp.1256.

Shepherd, R. G. (1972), Incised river meanders: Evolution in simulated bedrock, *Science*, *178*, 409–411, doi:10.1126/science.178.4059.409.

Shepherd, R. G., and S. A. Schumm (1974), Experimental study of river incision, *Geol. Soc. Am. Bull.*, *85*, 257–268, doi:10.1130/0016-7606(1974)85<257:ESORI>2.0.CO;2.

Singh, A., K. Fienberg, D. J. Jerolmack, J. Marr, and E. Foufoula-Georgiou (2009), Experimental evidence for statistical scaling and intermittency in sediment transport rates, *J. Geophys. Res.*, *114*, F01025, doi:10.1029/2007JF000963.

Sklar, L. S., and W. E. Dietrich (2001), Sediment and rock strength controls on river incision into bedrock, *Geology*, *29*, 1087–1090, doi:10.1130/0091-7613(2001)029<1087:SARSCO>2.0.CO;2.

Sklar, L. S., and W. E. Dietrich (2004), A mechanistic model for river incision into bedrock by saltating bed load, *Water Resour. Res.*, *40*, W06301, doi:10.1029/2003WR002496.

Stock, J. D., D. R. Montgomery, B. D. Collines, W. E. Dietrich, and L. Sklar (2005), Field measurements of incision rates following bedrock exposure: Implications for process controls on the long profiles of valleys cut by rivers and debris flows, *Geol. Soc. Am. Bull.*, *117*, 174–194, doi:10.1130/B25560.1.

Turowski, J. M. (2009), Stochastic modeling of the cover effect and bedrock erosion, *Water Resour. Res.*, *45*, W03422, doi:10.1029/2008WR007262.

Turowski, J. M., D. Lague, and N. Hovius (2007), Cover effect in bedrock abrasion: A new derivation and its implications for the modeling of bedrock channel morphology, *J. Geophys. Res.*, *112*, F04006, doi:10.1029/2006JF000697.

Turowski, J. M., N. Hovius, A. Wilson, and M. J. Horng (2008a), Hydraulic geometry, river sediment and the definition of bedrock channels, *Geomorphology*, *99*, 26–38, doi:10.1016/j.geomorph.2007.10.001.

Turowski, J. M., N. Hovius, H. Meng-Long, D. Lague, and C. Men-Chiang (2008b), Distribution of erosion across bedrock channels, *Earth Surf. Processes Landforms*, *33*, 353–363, doi:10.1002/esp.1559.

Turowski, J. M., D. Rickenmann, and S. J. Dadson (2010), The partitioning of the total sediment load of a river into suspended load and bedload: A review of empirical data, *Sedimentology*, *57*, 1126–1146, doi:10.1111/j.1365-3091.2009.01140.x.

Wallinga, J. (2002), Optically stimulated luminescence dating of fluvial deposits: A review, *Boreas*, *31*, 303–322, doi:10.1080/030094802320942536.

Whipple, K. X., G. S. Hancock, and R. S. Anderson (2000), River incision into bedrock: Mechanics and relative efficacy of plucking, abrasion, and cavitation, *Geol. Soc. Am. Bull.*, *112*, 490–503, doi:10.1130/0016-7606(2000)112<490:RIIBMA>2.0.CO;2.

Wolman, M. G. (1954), A method of sampling coarse river-bed material, *Trans. AGU*, *35*(6), 951–956.

Wong, M., and G. Parker (2006), Reanalysis and correction of bed-load relation of Meyer-Peter and Müller using their own database, *J. Hydrol. Eng.*, *132*, 1159–1169, doi:10.1061/(ASCE)0733-9429(2006)132:11(1159).

Wu, C. C., and Y. H. Kuo (1999), Typhoons affecting Taiwan: Current understanding and future challenges, *Bull. Am. Meteorol. Soc.*, *80*, 67–80, doi:10.1175/1520-0477(1999)080<0067:TATCUA>2.0.CO;2.

Yanites, B. J., and G. E. Tucker (2010), Controls and limits on bedrock channel geometry, *J. Geophys. Res.*, *115*, F04019, doi:10.1029/2009JF001601.

Yanites, B. J., G. E. Tucker, K. Mueller, Y. G. Chen, T. Wilcox, and S. Y. Huang (2010a), Incision and channel morphology across active structures in the Peikang River, central Taiwan: Implications for the importance of channel width, *Geol. Soc. Am. Bull.*, *122*, 1192–1208, doi:10.1130/B30035.1.

Yanites, B. J., G. E. Tucker, K. Mueller, and Y. G. Chen (2010b), How rivers react to large earthquakes: Evidence from central Taiwan, *Geology*, *38*, 639–642, doi:10.1130/G30883.1.

C. Chen and H.-L. Hsu, Institute of Geophysics, National Central University, 300 Jung-da Rd., Jhongli, Taoyuan 320, Taiwan.

Y.-G. Chen, Department of Geosciences, National Taiwan University, 1, Sec. 4 Roosevelt Rd., Taipei 106, Taiwan.

K. J. Mueller and G. E. Tucker, Department of Geological Sciences, University of Colorado at Boulder, 2200 Colorado Ave., Campus Box 399, Boulder, CO 80309-0399, USA.

B. J. Yanites, Department of Geological Sciences, University of Michigan, Rm. 2534, C.C. Little Bldg., 1100 N. University Ave., Ann Arbor, MI 48109, USA. (yanites@umich.edu)